ACS Medicinal Chemistry Letters

Letter

pubs.acs.org/acsmedchemlett

A-Ring Dihalogenation Increases the Cellular Activity of Combretastatin-Templated Tetrazoles

Thomas M. Beale,[†] Daniel M. Allwood,[†] Andreas Bender,[‡] Peter J. Bond,[‡] James D. Brenton,[§] D. Stephen Charnock-Jones,[∥] Steven V. Ley,[†] Rebecca M. Myers,*[,†] James W. Shearman,[†] Jill Temple,[§] Jessica Unger,[§] Ciorsdaidh A. Watts,[†] and Jian Xian[§]

[†]Department of Chemistry, Lensfield Road, University of Cambridge, Cambridge CB2 1EW, U.K.

[‡]Unilever Centre for Molecular Science Informatics, Lensfield Road, University of Cambridge, Cambridge CB2 1EW, U.K.

[§]Functional Genomics of Ovarian Cancer Laboratory, Cancer Research U.K., Cambridge Research Institute, Li Ka Shing Centre, Robinson Way, Cambridge CB2 0RE, U.K.

[∥]Department of Obstetrics and Gynaecology, University of Cambridge, and National Institute for Health Research, Cambridge Comprehensive Biomedical Research Centre, Cambridge CB2 0SW, U.K.

Supporting Information

ABSTRACT: The combretastatins have been investigated for their antimitotic and antivascular properties, and it is widely postulated that a 3,4,5-trimethoxyaryl A-ring is essential to maintain potent activity. We have synthesized new tetrazole analogues (**32**–**34**), demonstrating that 3,5-dihalogenation can consistently increase potency by up to 5-fold when compared to the equivalent trimethoxy compound on human umbilical vein endothelial cells (HUVECs) and a range of cancer cells. Moreover, this increased potency offsets that lost by installing the tetrazole bridge into combretastatin A-4 (**1**), giving crystalline, soluble compounds that have low nanomolar activity, arrest cells in G_2/M phase, and retain microtubule inhibitory activity. Molecular modeling has shown that optimized packing within the binding site resulting in increased Coulombic interaction may be responsible for this improved activity.

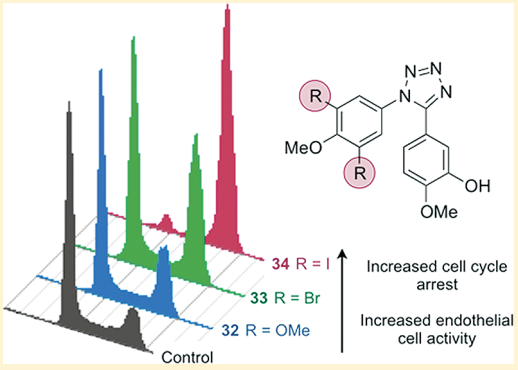

KEYWORDS: *Combretastatin, tetrazole, dihalogenation, human umbilical vein endothelial cell, ovarian cancer, vascular disrupting agent*

Combretastatin A-4 (CA-4) (**1**) isolated from the African willow tree, *Combretum caffrum*,[1] binds to the colchicine binding site on β-tubulin.[2] At nanomolar concentrations, it stabilizes the dynamics of cellular microtubules, arresting the cell cycle in metaphase and triggering apoptosis.[3] It is also a potent vascular disrupting agent (VDA). It is this property that has made **1** an attractive lead for the development of new anticancer therapies, since *in vivo* it readily cuts off blood supply to tumors.[4,5] Such is the interest in **1** that several structurally related VDAs are in clinical trials: the phosphate prodrug of **1** (Zybrestat, **2**), the phosphate prodrug of combretastatin A-1 (**3**), OXi4503 (**4**), and a serine prodrug (Ombrabulin, **5**) of a 3-amino CA-4 analogue (**6**) (Figure 1).[6−8] The syntheses and biological activities of combretastatin analogues have been reviewed, and what emerges from this literature is an intriguing correlation.[9−12] Almost without exception, the shared structural feature present in combretastatin analogues is a 3,4,5-trimethoxyaryl ring (A-ring), which is widely accepted to be essential for biological activity. However, we and others have recently reported that this is not necessarily the case (Figure 1).[13−17] In our recent work, we modified the A-ring of **1** and discovered that 3,5-dibromo- (**7**) and 3,5-diiodo- (**8**) substitution of the A-ring maintained, and even improved upon, the activity of **1** in human umbilical vein endothelial cells (HUVECs) and ovarian cancer cells (SK-OV-3 and paclitaxel-resistant SK-OV-3TR) (Figure 1).[13]

Cell cycle analysis of SK-OV-3 cells treated with 5 nM **7** and **8** indicated that a higher percentage of cells were arrested at the G_2/M phase: 52% and 84%, respectively, when compared to cells treated with **1** (31%).[13] These encouraging results led us to look at additional chemical improvements that could be made. We envisaged replacing the double bond with a tetrazole to mitigate the solubility problems of the *cis*-stilbenes in aqueous media and address the tendency of the most potent compound in the series (**8**) to isomerize in solution.[18] The few reports of tetrazole-containing VDAs have structures based on the template of **1**. For instance, direct replacement of the double bond in **6** with a tetrazole ring resulted in a compound

Received: June 22, 2011
Accepted: January 19, 2012
Published: January 19, 2012

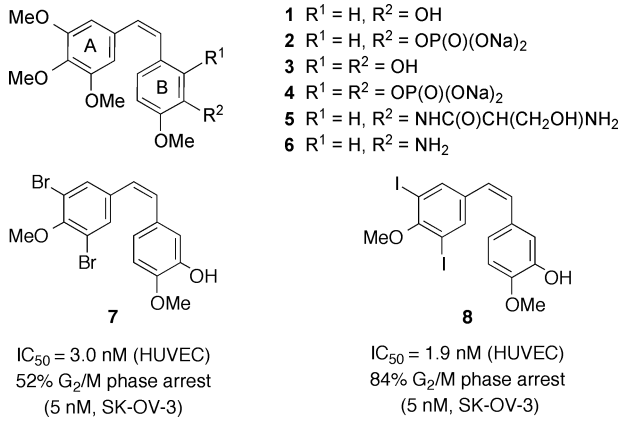

Figure 1. Combretastatin A-4 (**1**) and A-1 (**3**) and analogues in clinical trials. Dihalogenated A-ring analogues **7** and **8**.[13]

with nanomolar activity (IC_{50} = 7.2 nM) on colon 26 cells that maintained antitubulin activity (IC_{50} = 2 μM).[19] Replacement of the double bond in chalcone analogues with a tetrazole resulted in compounds with low micromolar activity (IC_{50} = 4.1 μM) on neuroblastoma SH-SY5Y cells.[20]

Our general approach for synthesis of tetrazoles **32**−**34** was to perform an amide coupling reaction between A-ring anilines and a B-ring acid derivative. Conversion of the resulting amides into thioamides and tetrazole formation using trimethylsilyl azide in the presence of mercury(II) acetate were envisaged as key steps toward the desired compounds (Scheme 1).

3,5-Dibromo-4-methoxy aniline (**12**) was obtained from **9** in 77% yield *via* acetyl protection of amine **9**, phenol methylation, and subsequent deacetylation. Iodination of 4-nitrophenol (**13**) using iodine monochloride formed *in situ* from sodium chlorite and sodium iodide gave **14**.[21] Treatment of **14** with dimethyl sulfate and potassium carbonate in refluxing acetone gave **15**, which was reduced using tin chloride in ethyl acetate and ethanol to give 3,5-diiodo-4-methoxyaniline (**16**) in 79% yield. Benzoic acid **19**, its ethyl carbonic anhydride derivative **20**, or its acid fluoride **21** were investigated as B-ring coupling partners. Acid **19** was obtained from *tert*-butyldimethylsilyl (TBDMS) protection of **17** in 39% yield or from aldehyde **18** *via* a two-step sequence of silyl protection and then aldehyde oxidation with copper(I) in 82% yield; **19** was transformed into **20** using ethyl chloroformate, or alternatively into **21** using cyanuric fluoride. After screening various coupling conditions, the optimal procedure for the synthesis of **23** was found to be diisopropylcarbodiimide (DIC) and *N*-hydroxybenzotriazole (HOBt). For **24** and **25** it was found that treatment of anilines **12** and **16** with sodium hydride followed by **20** gave the best results. Amides **23**−**25** were converted into their corresponding thioamides **26**−**28** using Lawesson's reagent. These were then treated with mercury(II) acetate in the presence of trimethylsilyl azide ($TMSN_3$) to give **29**−**31** through a one-pot desulfuration and cyclization reaction. After silyl protecting group removal, tetrazoles **32**−**34** were obtained in 48%, 30%, and 20% overall yield, respectively.

Using cancer cell lines and primary vascular endothelial cells, we investigated the effects of **32**−**34** on cell growth and on the cell cycle. We also observed their effects on isolated tubulin polymerization. Sulforhodamine B (SRB) assays were performed on six human carcinoma cell lines using three replicate experiments with errors shown as 95% confidence intervals (CI) (Table 1). In summary, **32**−**34** had low nanomolar

Scheme 1. Synthesis of Tetrazoles 32−34[a]

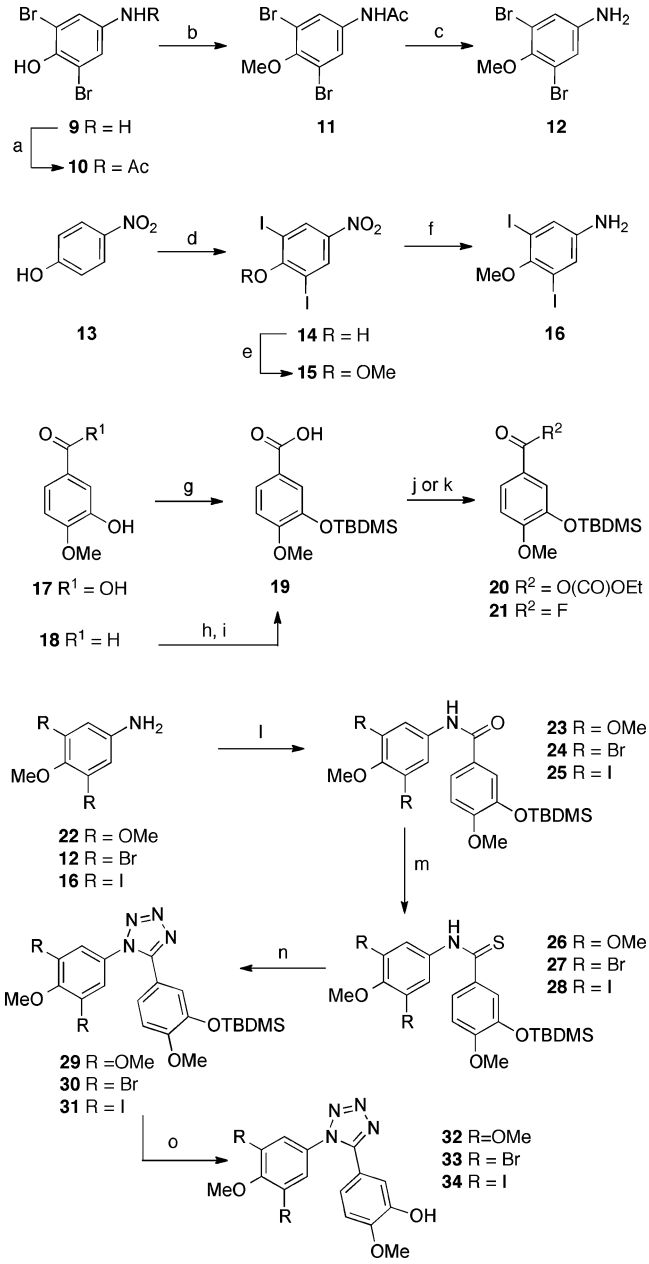

[a]Reagents and conditions: (a) Ac_2O, AcOH, rt, 30 min, 98%; (b) MeI, K_2CO_3, acetone, 120 °C, μW, 30 min, 83%; (c) 3 M HCl, 140 °C, μW, 10 min, 95%; (d) $NaClO_2$, NaI, HCl, MeOH/H_2O, 0 °C to rt, 18 h, 94%; (e) $(MeO)_2SO_2$, K_2CO_3, acetone, 65 °C, 18 h, 87%; (f) $SnCl_2$, EtOH/EtOAc, 70 °C, 2 h, 79%; (g) NaH, THF, 0 °C then TBDMSCl, 39%; (h) TBDMSCl, Et_3N, DMF, rt, 16 h, 97%; (i) 5 mol % CuCl, *t*-BuOOH, MeCN, 24 h, rt, 85%; (j) For **20**, ethyl chloroformate, NEt_3, THF, 0 °C to rt, 1 h, 98%; (k) For **21**, cyanuric fluoride, py, THF, −20 to 0 °C, 2 h, 99%; (l) For **23**, DIC, HOBt, **19**, CH_2Cl_2, DMF, 60 °C, μW, 30 min, 70%. For **24**, NaH, THF, 0 °C, then **20**, THF, rt, 18 h 44%. For **25**, NaH, THF, 0 °C, then **20**, THF, rt, 18 h, 62%; (m) Lawesson's reagent, THF. For **26**, 17 h, 80 °C, 98%. For **27**, 4 h, 70 °C, 80%. For **28**, 4 h, 70 °C, 79%; (n) $Hg(OAc)_2$, $TMSN_3$, THF. For **29**, 0 °C, 3 h, 87%. For **30**, 0 °C, 1 h, 97%. For **31**, 0 °C, 3 h, 87%; (o) TBAF, THF, rt, 1 h; **32**, 81%; **33**, 80%; **34**, 68%.

activity (IC_{50} = 0.5−24 nM) on all cell lines, excepting combretastatin-resistant HT29 cells. These results were comparable to those of the reference compound **1** on the

dx.doi.org/10.1021/ml200149g | *ACS Med. Chem. Lett.* 2012, 3, 177−181

Table 1. Growth Inhibition Effects of 1 and 32−34 on Human Carcinoma and Fibroblast Cell Lines

	1 (CA-4)		**32** (OMe)		**33** (Br)		**34** (I)	
cell line	IC_{50}/nM	95% CI	IC_{50}/nM	95% CI	IC_{50}/nM	95% CI	IC_{50}/nM	95% CI
SK-OV-3	1.7	0.9−2.5	9.5	8.9−10	6.1	5.5−6.6	2.6	1.7−3.4
SK-OV-3TR	4.2	3.3−5.1	11	8.4−13	5.6	2.0−9.1	1.4	0.2−5.9
MCF-7	3.0	2.0−4.0	21	13−29	7.0	4.6−9.5	1.9	1.0−2.9
A549	7.9	7.1−8.8	22	17−28	21	16−27	2.8	2.4−3.3
PC3	2.9	1.8−4.1	9.0	8.1−9.8	2.9	2.5−3.3	0.5	0.4−0.7
DLD1	3.3	1.1−5.4	24	21−28	8.2	7.9−8.5	2.4	1.8−3.1
HT29	538	425−651	>500	–	>500	–	513	452−574
MRC5	2.8	0.1−5.7	12	8.7−15.8	5.7	4.5−6.9	2.2	0.0−7.2

same cell lines (IC_{50} = 1.7−7.9 nM) (Table 1). A general increase in potency was observed across **32**−**34** on all cell lines. Trimethoxy tetrazole **32** was consistently the least potent compound, dibrominated **33** was intermediate in potency, and diiodinated **34** was the most potent compound, in most cases more potent than CA-4 (**1**).

The potency of tetrazoles **32**−**34** was unaffected by the mechanism of resistance in a taxol-resistant cell line (SK-OV-3TR), previously shown to be MDR1 overexpression.[22] However, CA-4 (**1**) and tetrazoles **32**−**34** were affected by HT29 resistance, with potencies reduced by over 100-fold. The resistance of this cell line is mediated by drug glucuronidation and MRP efflux.[23] However, it has been recently shown that tumor drug resistance is not detrimental to combretastatin efficacy *in vivo* due to the predomination of antivascular effects.[24] The tetrazoles **32**−**34** also exhibited the same profile as **1** on MRC5 human fibroblasts but once again demonstrated that diiodination of the tetrazole series allows greater potency.

Cell cycle analysis on SK-OV-3 cells following treatment with **32**−**34** at 5 nM showed that G_2/M arrest was correlated with increasing potency of inhibition of cell growth (Figure 2). The

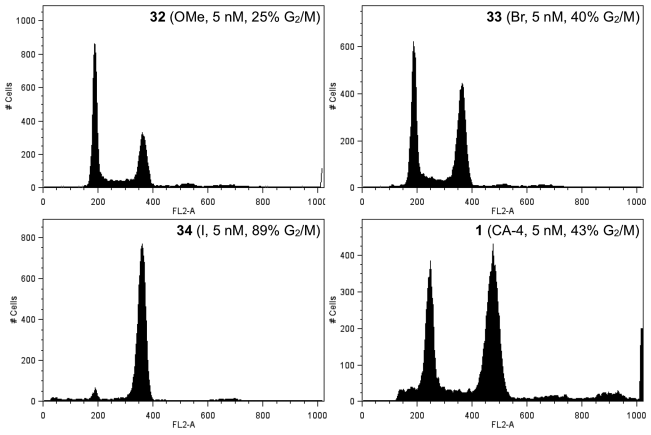

Figure 2. Cell cycle analysis for **32**−**34** at 5 nM on ovarian cancer cells (SK-OV-3).

percentage of cells in G_2/M increased from 25% for **32**, to 40% for **33**, to a maximum of 89% for the diiodinated tetrazole **34**. These results compare to 43% of cells in G_2/M for CA-4 (**1**) at 5 nM. In all cases, the percentage of sub-G_1 cells was less than 5%.

We then explored whether **32**−**34** could have therapeutic potential as VDAs. HUVECs are a model of tumor endothelium and can be used to evaluate antivascular effects of bioactive compounds. The results from treatment of HUVECs with **32**−**34** were obtained using the xCELLigence system, which gives a measure of cell number in real-time using impedance measurements (Table 2).

Table 2. Growth Inhibition Effects of 32−34 on HUVECs

	HUVEC 24 h IC_{50}/nM						
	isolate						
compd	1	2	3	4	5	6	mean
1 (CA-4)	1.9	2.2	–	2.2	2.3	–	2.2
32 (OMe)	10.0	–	20.4	9.9	21.4	6.5	13.6
33 (Br)	6.0	–	8.8	8.1	2.9	7.1	6.6
34 (I)	1.8	3.2	2.8	2.2	2.6	1.9	2.4

The average IC_{50} values on HUVECs reprise the results observed for the SK-OV-3 cell line; that is, potency increased from the trimethoxy compound **32** (IC_{50} = 13.6 nM), to **33** (IC_{50} = 6.6 nM) then **34** (IC_{50} = 2.4 nM), comparable to **1** (IC_{50} = 2.2 nM). The absolute values mirror those obtained on SK-OV-3 cells, suggesting **32**−**34** display no selectivity for vascular cells over carcinoma cells.

The effect of **32**−**34** and **1** on tubulin polymerization was also investigated. Compounds were tested at a concentration of 5 μM, and data is reported as the fold reduction in V_{max} relative to vehicle control averaged over four separate measurements ± standard deviation. Change in V_{max} was used, as it is the most sensitive indicator of tubulin/drug interactions. Compound **32** (2.9 ± 1.7) had very similar potency to **1** (3.0 ± 0.4), with both compounds able to reduce tubulin polymerization approximately 3-fold relative to control. Compounds **33** and **34** were less active, with 1.5 ± 0.4 and 1.7 ± 0.3 fold reduction in tubulin polymerization, respectively. The induction of microtubule depolymerization at this concentration suggests that these tetrazole compounds retain ability to bind at the colchicine-binding site on tubulin.

To further investigate the binding ability of **32**−**34** and to propose a rationale for the added potency of dihalogenated compounds **33** and **34** over **32**, we performed molecular modeling with tubulin (pdb: 1SA0)[25] (Table 3). The final interaction energies between protein and ligand consistently predicted that **32**−**34** bind in a single orientation analogous to that for **1** and colchicine, with the B-ring 3-hydroxyl picking up a key hydrogen bond with the backbone carbonyl of Thr179 and an interaction with the side chain ε-amino group of Lys350, as previously described for many combretastatin analogues.[26] It appears that in both **33** and **34** there is an additional interaction between the B-ring 4-methoxy oxygen and Lys350 that is not present for **32**.

The key difference between the calculated binding of **32**−**34** is in the position of the A-ring in the binding pocket and

dx.doi.org/10.1021/ml200149g | ACS Med. Chem. Lett. 2012, 3, 177−181

Table 3. Calculated Interaction Energies and Modeled Binding to Tubulin for Compounds 32−34 and Contribution from van der Waals and Coulombic Interactions (32 in Green, 33 in Cyan, and 34 in Magenta)

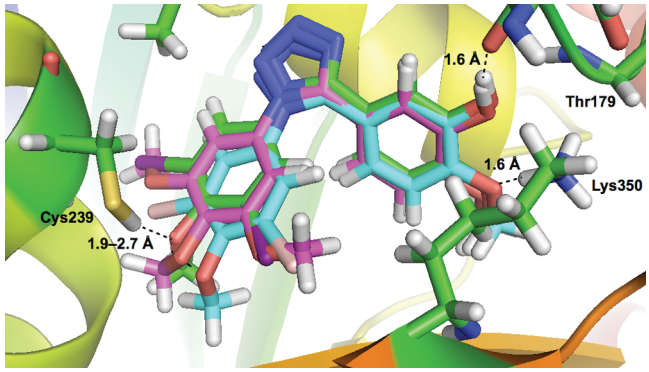

	binding energy/(kcal mol^{-1})		
compd	total	van der Waals	Coulombic
32 (OMe)	−83.19	−50.90	−32.29
33 (Br)	−83.38	−48.00	−35.38
34 (I)	−90.14	−49.55	−40.59

especially in the location of the 4-methoxy group relative to Cys239, which is the important hydrogen bonding interaction for this part of the molecule. For **34** the S−H···O distance is 1.9 Å, whereas for **32** and **33** this distance is longer, at 2.1 and 2.7 Å, respectively. This demonstrates an improved ability to hydrogen bond at this position for **34**, while **33** further suffers from a loss of electrostatic interaction in the tetrazole bridge region with the backbone amine of Ala248 that is maintained by diiodinated **34**. This is reinforced by the calculated interaction energies, which show that our most potent compound (**34**) is predicted to have the greatest energy of interaction (Table 3). Surprisingly, given the large size and polarizability of iodine, it is not a greater van der Waals interaction that gives this added interaction energy but rather that the optimal packing of **34** within the binding site results in improved electrostatic and hydrogen bonding interactions with protein residues.

Taken together, this data shows that substituting the double bond of CA-4 (**1**) with a tetrazole reduces cellular potency by 5- to 10-fold but that introduction of bromine or iodine atoms at the 3- and 5-positions of the A-ring can restore potency to the level of CA−4 (**1**). The tetrazoles are crystalline and chemically stable, which is not true for many stilbene-based combretastatin analogues, bringing obvious advantages. Molecular modeling shows that the enhanced activity of diiodinated compound **34** may be due to optimized packing into the colchicine binding site, resulting in greater electrostatic interactions with tubulin.

■ ASSOCIATED CONTENT

Ⓢ Supporting Information

Full experimental details for the synthesis of **32**, **33**, and **34** (including intermediates) with full characterization data; crystallographic data for **33**; and biological assay and computational methods. This material is available free of charge via the Internet at http://pubs.acs.org.

■ AUTHOR INFORMATION

Corresponding Author

*Telephone: +44 (0) 1223 336334. Fax: +44 (0) 1223 336442. E-mail: rmm32@cam.ac.uk.

Funding

T.M.B., J.W.S., D.M.A., and C.A.W. thank the CRUK Ph.D. Training Programme for Medicinal Chemistry for funding. P.J.B. and A.B. thank Unilever for funding. S.V.L. acknowledges support from the BP Endowment.

Notes

The authors declare no competing financial interest.

■ ACKNOWLEDGMENTS

The authors would like to thank Richard Farndale for use of the xCELLigence facilities at the Department of Biochemistry at the University of Cambridge. The computational work used the Darwin Supercomputer at the University of Cambridge High Performance Computing Service (http://www.hpc.cam.ac.uk/) provided by Dell Inc., using Strategic Research, Infrastructure Funding from the Higher Education Funding Council for England.

■ ABBREVIATIONS

HUVECs, human umbilical vein endothelial cells; CA-4, combretastatin A-4; VDA, vascular disrupting agent; TBDMS, *tert*-butyldimethylsilyl; DIC, diisopropylcarbodiimide; HOBt, *N*-hydroxybenzotriazole; TMS, trimethylsilyl; TBAF, tetrabutylammonium fluoride; SRB, sulforhodamine B; CI, confidence intervals

■ REFERENCES

(1) Pettit, G. R.; Singh, S. B.; Hamel, E.; Lin, C. M.; Alberts, D. S.; Garcia-Kendall, D. Isolation and structure of the strong cell growth and tubulin inhibitor combretastatin A-4. *Experientia* **1989**, *45*, 209−211.

(2) Lin, C. M.; Ho, H. H.; Pettit, G. R.; Hamel, E. Antimitotic natural products combretastatin A-4 and combretastatin A-2: studies on the mechanism of their inhibition of the binding of colchicine to tubulin. *Biochemistry* **1989**, *28*, 6984−6991.

(3) Cushman, M.; Nagarathnam, D.; Gopal, D.; He, H. M.; Lin, C. M.; Hamel, E. Synthesis and evaluation of analogues of (*Z*)-l-(4-methoxyphenyl)-2-(3,4,5-trimethoxyphenyl)ethene as potential cytotoxic and antimitotic agents. *J. Med. Chem.* **1992**, *35*, 2293−2306.

(4) Dark, G. G.; Hill, S. A.; Prise, V. E.; Tozer, G. M.; Pettit, G. R.; Chaplin, D. J. Combretastatin A-4, an agent that displays potent and selective toxicity toward tumor vasculature. *Cancer Res.* **1997**, *57*, 1829−1834.

(5) Thorpe, P. E. Vascular Targeting Agents as Cancer Therapeutics. *Clin. Cancer Res.* **2004**, *10*, 415−427.

(6) Dumontet, C.; Jordan, M. A. Microtubule-binding agents: a dynamic field of cancer therapeutics. *Nat. Rev. Drug Discovery* **2010**, *9*, 790−803.

(7) Cai, X. Small molecule vascular disrupting agents: potential new drugs for cancer treatment. *Recent Pat. Anti-Cancer Drug Discovery* **2007**, *2*, 79−101.

(8) Hinnen, P.; Eskens, F. Vascular disrupting agents in clinical development. *Br. J. Cancer* **2007**, *96*, 1159−1165.

(9) Singh, S. R.; Kaur, H. Advances in synthetic approaches for the preparation of combretastatin-based anti-cancer agents. *Synthesis* **2009**, 2471−2491.

(10) Tron, G. C.; Pirali, T.; Sorba, G.; Pagliai, F.; Busacca, S.; Genazzani, A. A. Medicinal chemistry of combretastatin A-4: present and future directions. *J. Med. Chem.* **2006**, *49*, 3033−3044.

(11) Shan, Y.; Zhang, J.; Liu, Z.; Wang, M.; Dong, Y. Developments of combretastatin A-4 derivatives as anticancer agents. *Curr. Med. Chem.* **2011**, *18*, 523−538.

(12) Bhattacharyya, B.; Panda, D.; Gupta, S.; Banerjee, M. Anti-mitotic activity of colchicine and the structural basis for its interaction with tubulin. *Med. Res. Rev.* **2008**, *28*, 155−183.
(13) Beale, T. M.; Myers, R. M.; Shearman, J. W.; Charnock-Jones, D. S.; Brenton, J. D.; Gergely, F. V.; Ley, S. V. Antivascular and anticancer activity of dihalogenated A-ring analogues of combretastatin A-4. *Med. Chem. Commun.* **2010**, *1*, 202−208.
(14) Schobert, R.; Biersack, B.; Dietrich, A.; Effenberger, K.; Knauer, S.; Mueller, T. 4-(3-Halo/amino-4,5-dimethoxyphenyl)-5-aryloxazoles and -N-methylimidazoles that are cytotoxic against combretastatin A resistant tumor cells and vascular disrupting in a cisplatin resistant germ cell tumor. *J. Med. Chem.* **2010**, *53*, 6595−6602.
(15) Pettit, G. R.; Minardi, M. D.; Rosenberg, H. J.; Hamel, E.; Bibby, M. C.; Martin, S. W.; Jung, M. K.; Pettit, R. K.; Cuthbertson, T. J.; Chapuis, J.-C. C. Antineoplastic agents. 509. Synthesis of fluorcombstatin phosphate and related 3-halostilbenes. *J. Nat. Prod.* **2005**, *68*, 1450−1458.
(16) Simoni, D.; Romagnoli, R.; Baruchello, R.; Rondanin, R.; Grisolia, G.; Eleopra, M.; Rizzi, M.; Tolomeo, M.; Giannini, G.; Alloatti, D. Novel A-ring and B-ring modified combretastatin A-4 (CA-4) analogues endowed with interesting cytotoxic activity. *J. Med. Chem.* **2008**, *51*, 6211−6215.
(17) Gaukroger, K.; Hadfield, J. A.; Lawrence, N. J.; Nolan, S.; McGown, A. T. Structural requirements for the interaction of combretastatins with tubulin: how important is the trimethoxy unit? *Org. Biomol. Chem.* **2003**, *1*, 3033−3037.
(18) Isomerization was observed by ^{1}H NMR spectroscopy when a sample of **8** had been standing in $CDCl_3$ over several days.
(19) Ohsumi, K.; Hatanaka, T.; Fujita, K.; Nakagawa, R.; Fukuda, Y.; Nihei, Y.; Suga, Y.; Morinaga, Y.; Akiyama, Y.; Tsuji, T. Syntheses and antitumor activity of *cis*-restricted combretastatins: 5-membered heterocyclic analogues. *Bioorg. Med. Chem. Lett.* **1998**, *8*, 3153−3158.
(20) Mesenzani, O.; Massarotti, A.; Giustiniano, M.; Pirali, T.; Bevilacqua, V.; Caldarelli, A.; Canonico, P.; Sorba, G.; Novellino, E.; Genazzani, A. A.; Tron, G. C. Replacement of the double bond of antitubulin chalcones with triazoles and tetrazoles: synthesis and biological evaluation. *Bioorg. Med. Chem. Lett.* **2011**, *21*, 764−768.
(21) Lista, L.; Pezzella, A.; Napolitano, A.; d'Ischia, M. Mild and efficient iodination of aromatic and heterocyclic compounds with the $NaClO_2$/NaI/HCl system. *Tetrahedron* **2008**, *64*, 234−239.
(22) Duan, Z.; Feller, A. J.; Toh, H. C.; Makastorsis, T.; Seiden, M. V. TRAG-3, a novel gene, isolated from a taxol-resistant ovarian carcinoma cell line. *Gene* **1999**, *229*, 75−81.
(23) Cummings, J.; Zelcer, N.; Allen, J.; Yao, D.; Boyd, G.; Maliepaard, M.; Friedberg, T.; Smyth, J.; Jodrell, D. Glucuronidation as a mechanism of intrinsic drug resistance in colon cancer cells: contribution of drug transport proteins. *Biochem. Pharmacol.* **2004**, *67*, 31−39.
(24) Lunt, S. J.; Akerman, S.; Hill, S. A.; Fisher, M.; Wright, V. J.; Reyes-Aldasoro, C. C.; Tozer, G. M.; Kanthou, C. Vascular effects dominate solid tumor response to treatment with combretastatin A-4-phosphate. *Int. J. Cancer* **2011**, *129*, 1979−1989.
(25) Ravelli, R. B.; Gigant, B.; Curmi, P. A.; Jourdain, I.; Lachkar, S.; Sobel, A.; Knossow, M. Insight into tubulin regulation from a complex with colchicine and a stathmin-like domain. *Nature* **2004**, *428*, 198−202.
(26) Botta, M.; Forli, S; Magnani, M.; Manetti, F. Molecular modeling approaches to study the binding mode on tubulin of microtubule destabilizing and stabilizing agents. *Top. Curr. Chem.* **2009**, *286*, 279−328.